Physically Representative Network Models of Transport in Porous Media

Steven L. Bryant, David W. Mellor, and Christopher A. Cade
BP Research, Sunbury-on-Thames, Middlesex TW16 7LN, U.K.

We calculate permeabilities for a class of granular porous media derived from a real, disordered packing of equal spheres. The entire structure, including pore space, of these media is completely specified by the radii and spatial locations of the constituent grains. When geometric nearest neighbor grains are grouped together, the structure may be subdivided into pore bodies and pore throats in a natural and unambiguous way. From this subdivision we can establish a network of flow paths whose geometry and topology are completely specified, so that permeability and other transport coefficients can be calculated directly and without any adjustable parameters. The calculations focus on processes that form porous media, rather than on specific examples of such media. Hence, the approach is essentially predictive, rather than correlative. No additional measurements (such as capillary pressure data or pore system data from thin sections) are required, and correlations between permeability and other properties are not used. Predicted permeabilities match measurements on sandstone samples similar to the model porous media studied here over a wide range of porosity. Geometrical attributes of the network representation of the pore space of the model media are found to be spatially correlated. This departure from randomness significantly affects permeability. The agreement between predictions and measurements suggests that spatial correlation is inherent in granular porous media and that uncorrelated network models are therefore unlikely to be physically representative of such media.

Introduction

The permeability of granular porous media is an important property in a variety of applications, ranging from packed-bed reactors to oil and gas production. Consequently, a number of approaches have been employed to predict permeability and to understand how it depends on the pore structure of granular media. One popular approach is the network model (Fatt, 1956), in which the pore space is represented as a graph of connected sites. A common interpretation of this graph is that the sites correspond to pore bodies, and the bonds correspond to pore throats connecting the pore bodies.

In principle, a network model can replicate both the geometry and topology of pore space, so that flow through the network is equivalent to flow through the actual porous medium. Direct replication, however, has proven elusive because the pore space in real granular media is complicated. Very few measurements of pore dimensions on actual networks have been attempted (Dullien and Dhawan, 1975; Lin and Cohen, 1982; Koplik et al., 1984; Yanuka et al., 1986; Wardlaw et al., 1987). In practice, therefore, network models are usually generated stochastically using frequency distributions of geometric features such as pore throat radii.

The application of stochastic networks raises several difficulties. First, such networks do not necessarily preserve the spatial allocation of geometrical features in real media. This is despite the fact that information on such allocation is often implicit in the measurement used to obtain the frequency distributions, such as analysis of images of 2D sections (Ehrlich et al., 1984; Doyen, 1988; Schlueter et al., 1990) or deconvolution of saturation vs. capillary pressure data (Payatakes et al., 1973; Mishra and Sharma, 1988; Spearing and Matthews, 1991). Furthermore, parameters such as pore lengths and net-

Correspondence concerning this article should be addressed to S. L. Bryant who is presently at BP Chemicals, Bo'ness Road, Grangemouth, Stirlingshire, FK3 9XH, U.K.

work connectivity are difficult to measure, and frequently they are assigned arbitrary values or treated as adjustable parameters. Thus, even if the calculated network permeability matches the measured permeability for a particular medium, the network does not necessarily replicate the pore space of the medium. As a result, the network may not be appropriate for studying transport properties other than permeability, such as diffusivity or electrical conductivity. A too literal acceptance of such networks may also lead to incorrect conclusions regarding the structure of pore space.

A particular disadvantage of stochastically generated networks is that the frequency distributions and any adjustable parameters used are usually specific to one porous medium. While measuring these distributions increases the understanding of the particular sample, rigorous extrapolation of the resulting network model to other porous media is rarely possible. This is a serious drawback if the goal is to predict properties of porous media when detailed measurements on samples are not available or to understand how physical processes that create porous media influence their properties. These goals can have useful application in areas such as predicting permeability and porosity in oil exploration and designing the properties of packed beds or composite materials.

In this article, we present a new method of obtaining network models of pore space in consolidated granular media. Starting with a real, densely packed, unconsolidated collection of equal spheres, we simulate the results of certain physical processes that form consolidated porous media. The structure of the simulated media is completely determined, so we can extract network models directly from this structure. Transport properties such as permeability can then be calculated from the networks in the usual way. This approach circumvents the practical difficulties in obtaining detailed measurements of pore space in particular samples, as well as the theoretical difficulties in constructing a physically representative model from such measurements. The power of this approach for certain geological applications was previously demonstrated by Roberts and Schwartz (1985) and Schwartz and Banavar (1989). The present work was conceived and conducted independently and thus differs from previous work in several important aspects, though the essential idea of focusing on processes rather than objects is the same.

A process-based approach offers several advantages over conventional approaches. First, the model porous media are derived from a real, well-characterized, monodisperse granular packing. Though idealized, they are physically representative. This permits direct physical insight into the influence of various factors on permeability. It also permits direct and independent calculation of other transport properties such as diffusivity, electrical conductivity, and relative permeabilities. Second, the approach is physically rigorous. No adjustable parameters enter the calculations. The geometry of the model determines all pore space features, including parameters such as connectivity that are difficult to measure in samples. Finally, the approach is predictive, as opposed to correlative. This is because the input data can be derived from knowledge of the processes that formed the porous media. For the simple class of granular media considered here, these data are minimal (porosity and, if a length scale is required, grain size). No additional measurements of any kind are required.

The rules for creating the class of granular media presented here are designed to simulate certain geological processes (grain packing, compaction, and grain growth) involved in the formation of sandstones. However, because our treatment focuses on the results of these processes, rather than the detailed mechanisms that underly the processes, it is not limited to geological applications. Indeed, analogous processes occur in diverse areas such as sintering and hot-pressing (Lange and Kellett, 1989; Fernandez et al., 1991; Sung et al., 1991), recrystallization (Vandermeer et al., 1991), fabrication of composite materials (Currier, 1990; Tai and Chou, 1990; Lange et al., 1991; Chung et al., 1991), biological growth in soils (Taylor et al., 1990), and fine particle filtration (De Cayeux et al., 1990; Rege and Fogler, 1988). Grain growth/shrinking also occurs in a number of fluid/solid reactions including gas desulfurization, dissolution/precipitation of solids by acid, coal gasification, and catalyst deactivation (Yu and Sotirchos, 1987; Sotirchos and Zarkanitis, 1989; Alvfors and Svedberg, 1992; see especially the review by Sahimi et al., 1990).

We begin by describing the construction of a simple class of porous media from a well-known dense random packing of equal spheres. Next, we describe properties of these media deduced from a faithful network representation of their pore space. The predicted permeabilities are compared with published measurements on some 200 samples of Fontainebleau sandstone. Finally, we discuss physical insights obtained from the model.

A Two-Parameter Class of Granular Porous Media

Figure 1 depicts three processes that contribute to the formation of granular media: sedimentation, compaction, and grain growth. Here, the term sedimentation means the accumulation or creation of a close packing of grains. Compaction means the mechanical compression of the packing, which reduces the bulk volume of the packing and causes the grains to move relative to each other. The movements typically result in grain interpenetration (by pressure solution, for example) and/or deformation, but we assume that no grain fracturing occurs. Grain growth causes the radii of the grains to increase without changing the relative positions of the grain centers. Grain growth may be viewed as the deposition of a film on all available surface of the pore space, as would occur during precipitation or crystallization of some cementing phases, for example.

We simulate here only the results of these processes, not the mechanisms by which the processes take place. This maintains some generality in the treatment at the expense of being able to relate process dynamics to macroscopic properties. For example, we will be able to predict the permeability of a packing after a given volume of material has been uniformly deposited within the packing, but we will not be concerned with the convection, diffusion and precipitation processes that may have introduced the material into the packing.

Sedimentation

Our starting point is a dense random packing of equal spheres. Finney (1968, 1970) constructed such a packing and measured the spatial coordinates of the centers of some 8,000 spheres therein. This information completely specifies the geometry of both the grain space and the pore space. We are aware of no other real, disordered granular medium for which

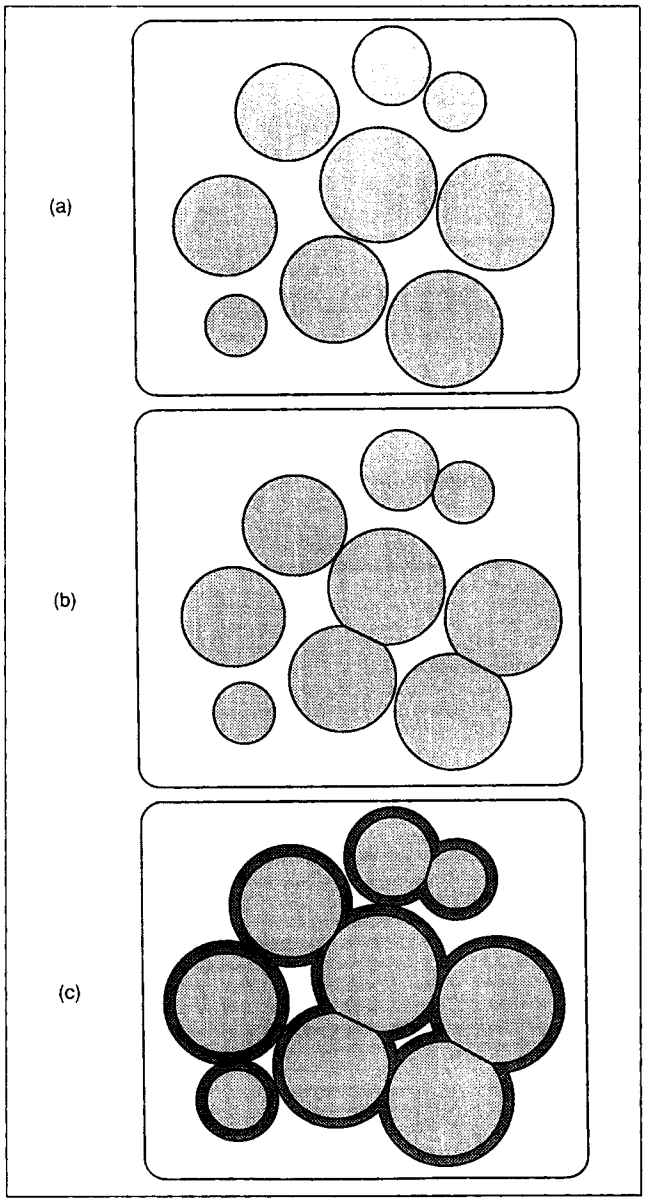

Figure 1. Formation of a two-parameter class of granular media.

(a) 2-D slice through a dense packing of equal spheres; (b) compaction (Eq. 1) forces spheres closer together and interpenetration occurs; (c) grain growth (Eq. 2) increases the radii of all the spheres.

a macroscopic volume has been so thoroughly characterized. A dense random sphere pack is a reasonable idealization of a sediment of sand grains in a wide spectrum of natural depositional environments. Such a packing may also be used to represent a powder prior to sintering or pressing or a clean filter medium.

Compaction

We consider compaction in one axial direction, for example, as it occurs when a sand body is buried to depths of several kilometers in the earth's crust, or when powders are fused under axial confining pressure. Numerically this is equivalent to rescaling one of the coordinate axes, x_j, used for Finney's measurements by the formula:

$$x_j' = x_{j_0} + \lambda (x_j - x_{j_0}) \tag{1}$$

where x_{j_0} is an arbitrary reference value and λ quantifies the degree of compaction. (The Finney packing is isotropic, so the choice of axis in Eq. 1 is arbitrary. In this article, we apply Eq. 1 to the x_3 axis.) For our geological applications, a physically reasonable range for λ is $0.7 < \lambda < 1.0$, corresponding to a range of 30% to 0% decrease in bulk volume. The coordinate transformation, Eq. 1, moves the sphere centers closer together and thus causes individual sphere spaces to interpenetrate. For simplicity, we assume that interpenetration causes no deformation, so that the grains remain perfectly spherical. In effect, this assumption is equivalent to pressure solution at grain contacts. The volume of grain interpenetration ($\equiv$ pressure-dissolved material) can be exported from the packing, or it can be redistributed in the packing, depending on the underlying physical mechanisms of interest. In this article, we choose to export the volume from the packing.

Grain growth

A variety of mechanisms can cause grains to grow. A geological example is quartz cementation. As pore fluid chemistry evolves in a buried sand body, quartz may precipitate on grain surfaces. The precipitated quartz often forms approximately concentric rims on the sand grains. Other examples of grain growth are relocation of material during sintering, deposition of secondary material in a composite, adhesion of small particles to grains in a filter, and conversion of $CaCO_3$ to $CaSO_4$ in gas desulfurization by limestone. To simulate grain growth, we increase the radius of the spheres in the packing without altering the location of the sphere centers:

$$R_i' = R_i + \Delta R \tag{2}$$

where R_i is the radius of the ith sphere. Although no fundamental difficulties arise if the grains grow by different increments, for simplicity we assume here that all grains grow uniformly, that is, the same value of ΔR applies for all i in Eq. 2. In many situations, this is a reasonable assumption, at least at the length scale of our packing ($\sim$20 grain diameters). Such uniform "grain consolidation" has been used to study the effect of cementation on electrical conductivity of rocks (Roberts and Schwartz, 1985; Schwartz and Kimminau, 1987). The grain growth may be reversed ($\Delta R < 0$) to simulate processes such as coal gasification, acid dissolution of minerals, or transfer of material from one grain to another, though we do not show this here.

When applied to Finney's measured sphere center coordinates, Eqs. 1 and 2 define a family of media involving two parameters, ΔR and λ. This class of granular media may also be viewed as a special case of a dense collection of randomly located overlapping spheres (Elam et al., 1984; Rubinstein and Torquato, 1989). Such collections are effectively a one-parameter family (the one parameter being the degree of sphere overlap permitted), and they can be readily created using computers. However, it is not trivial to generate large numerical

packings that reproduce the features of Finney's real packing. Also, it is somewhat more direct to simulate the distinct processes of grain growth and compaction with ΔR and λ than with the single parameter of permitted sphere overlap. For these reasons, we prefer to use the Finney packing as the basis for developing model porous media.

Properties of the Two-Parameter Class of Porous Media

Permeability and porosity

Our calculation of permeability and porosity in this class of granular media employs a network model of the pore space. The details of the calculation for the case of the uncompacted, uncemented Finney packing ($\Delta R = 0$, $\lambda = 1$) have been described elsewhere (Bryant et al., 1993). Because the extension to compacted/cemented packings is straightforward, only a summary of the procedure is given in the Appendix. Two key features emerge. First, no adjustable parameters enter the calculations, and no supplementary measurements are required. This is because the topology and geometry of the network model are completely determined by the locations and radii of the spheres in the packing. Thus, the network model faithfully reproduces the actual pore space of the media. Second, the network exhibits spatial correlation at the pore scale, and this departure from randomness significantly influences macroscopic properties.

Figure 2 shows the permeability of this class of granular media as a function of porosity for three cases: when only compaction occurs, when only grain growth occurs, and when 20% compaction is followed by grain growth. Each curve originates at $\phi = 0.362$, the porosity of the original Finney packing. The permeability of the original packing, denoted k_0, is used to normalize the permeabilities of the packings after compaction and/or grain growth.

The compaction-only curve in Figure 2 is obtained by applying Eq. 1 to the sphere center coordinates of the original Finney packing using different values of λ from the range $0.5 < \lambda < 1.0$. Using $\lambda = 1$ does not change the relative sphere locations and hence corresponds to the original Finney packing; decreasing λ corresponds to moving left along the curve in Figure 2. The sphere centers are forced closer together as λ decreases, but the sphere radii are constant and equal to their original value. Permeability and porosity are calculated as described in the Appendix for each value of λ.

The grain-growth-only curve is obtained by applying Eq. 2 recursively with small increments ΔR. Using $\Delta R = 0$ does not change the sphere size and hence corresponds to the original Finney packing; adding positive increments ΔR to the sphere size corresponds to moving left along the curve in Figure 2. The sphere centers remain at their original locations during grain growth. After each increment is added to the sphere radii, the permeability and porosity are calculated. Grain growth was halted slightly above the percolation threshold (see below), when $R_i' \sim 1.26 R_0$.

The combined compaction/grain-growth curve in Figure 2 is intended to simulate the geological sequence of burying a sediment, then introducing quartz cement. Thus, it follows the compaction-only curve down to the permeability/porosity corresponding to 20% compaction ($\lambda = 0.8$), after which increments ΔR are successively added to the sphere radii.

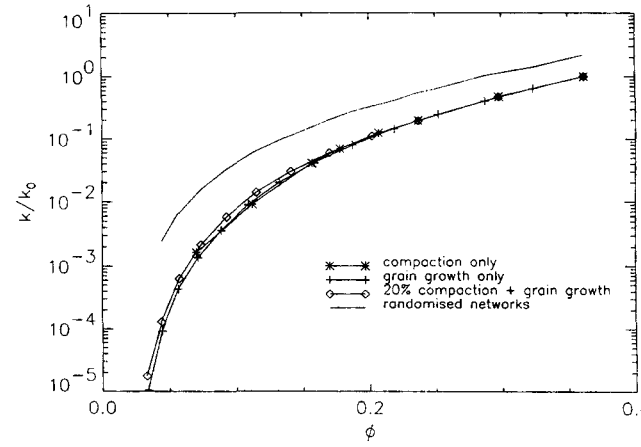

Figure 2. Although grain growth and compaction correspond to different physical processes, they produce remarkably similar permeability/porosity trends.

The calculated permeabilities are normalized to k_0, the permeability in the original Finney packing before grain growth or compaction start. Because the pore space is spatially correlated at the pore scale, random networks with the same topology and frequency distribution of conductivities have significantly higher permeabilities than the physically representative networks.

Although the mechanisms of compaction and grain growth are obviously different, their permeability/porosity trends nearly coincide. Curves for different degrees of compaction followed by grain growth exhibit the same trend. From this we conclude that the details of how compaction and grain growth combine to yield a particular porosity are not critical to determining the permeability in this simple class of porous media. Thus, porosity can be used as a single independent variable. This result perhaps would have been less surprising had we chosen to characterize this class of media with a single parameter (that is, the permitted degree of sphere overlap). This relationship lends some credence to the engineering practice of cross-plotting permeability and porosity, despite the fact that neither property is a simple function of the other in conventional theoretical treatments. We emphasize, however, that this result has been obtained in monodisperse media. We suspect that the trends may not coincide if the original grains are polydisperse.

Spatial correlation

The physical correspondence between a bond in the network and a particular flow path in the packing is crucial. This is because the hydraulic conductivities of the flow paths are found to be spatially correlated: *they are not distributed independently over the network*. This is a fundamental problem for advocates of stochastic models. In the original Finney packing, flow paths that are very close to each other tend to have similar conductivities (Bryant et al., 1993). A measure of the macroscopic effect of this pore-scale correlation can be obtained by comparison with uncorrelated networks having the same topology and frequency distribution of conductivities. Such networks are readily created by randomly reassigning the calculated conductivities in the physically representative networks. When this procedure is carried out for the original

Finney packing, the permeability of the network increases by a factor of 2.

In packings that have undergone compaction and/or grain growth, the effect of spatial correlation is magnified. We find that the permeability of a network constructed directly from the pore space of a compacted/cemented packing is always smaller than the permeability of an uncorrelated network having identical topology and frequency distribution of conductivities, as shown in Figure 2. The ratio of randomized network permeability to physically representative network permeability is 2 to 2.5 in lightly consolidated packings (porosity greater than 0.25) and 10 to 30 in heavily consolidated packings (porosity less than 0.075). This ratio diverges at the percolation threshold for physically representative networks (porosity ~ 0.03) because uncorrelated networks remain conductive at this point.

The selection of any method of identifying pore bodies in real porous media must remain arbitrary. Even the physically representative networks are merely convenient discretizations of the real pore space. Nevertheless it seems likely that spatial correlation is inherent in the packing rather than in the method of obtaining a network representation. Hence, we conclude that *networks of independently distributed conductivities are unlikely to be physically representative of the pore space in granular media.* A similar conclusion applies to networks of arbitrarily correlated conductivities. These conclusions are consistent with the results of Mason and Mellor (1991) for capillary transport and the results of Roberts and Schwartz (1985) for electrical transport.

Percolation

As porosity decreases due to compaction and grain growth, pore throats eventually become completely blocked, as shown in Figure 3. The blocking of pore throats introduces the phenomenon of bond percolation. As our networks are roughly spherical, it is convenient (but not rigorous) to associate bond percolation with the existence of a connected path between the central site in the network and the external boundary of the network. The threshold of percolation thus defined occurs at about 3% porosity, and at the threshold we find that 50% of the pore throats are blocked. These values agree with thresholds in the directions of the coordinate axes obtained (for grain growth only) by Roberts and Schwartz (1985) in a larger subset of Finney's packing. The porosity at the threshold also agrees with the value found for collections of overlapping randomly located spheres (Elam et al., 1984).

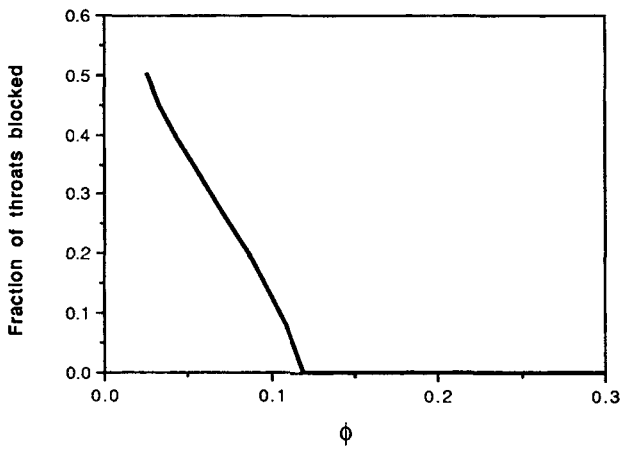

Figure 3. As λ decreases (increasing the degree of compaction) and Δ *R* increases (increasing the degree of grain growth), the porosity of the sphere packing decreases.

When the porosity reaches about 0.10, the smaller pore throats in the sphere packing become blocked. The percolation threshold occurs at a porosity of around 0.03 when 50% of the pore throats are blocked.

The fraction of blocked throats at the percolation threshold is significantly smaller than the value expected in random 3-D lattices of coordination four. If we block throats in our network randomly, rather than by simulating compaction/grain growth, we reach the percolation threshold when 61% of the throats are blocked. This value is the same as that for a random diamond lattice (Ripley, 1981). Topological correlation cannot account for the different thresholds, since the network representations of our model media are topologically disordered. Hence the difference between the threshold for our media and for random networks is another manifestation of pore scale spatial correlation in the media (Roberts and Schwartz, 1985; Mason and Mellor, 1991).

Comparison of Predictions with Measurements

The Fontainebleau sandstone is essentially pure quartz and is quarried near Paris in the Ile de France area. The distribution of grain sizes in this Oligocene rock is quite narrow, and the average grain size is nearly constant across the outcrop. However, the extent of quartz cementation in the outcrop varies widely, so that porosity and permeability vary widely as well. Because quartz cementation is reasonably approximated by uniform grain growth, this rock is comparable to the model granular media described above. It, therefore, provides a convenient test of the network representations of these model media.

Permeability has units of (length)^2, so comparison of the predictions presented above with measurements introduces a length scale. The natural length scale in our model is R_0, the initial radius of the spheres in the Finney packing. In terms of geological processes, this initial sphere radius corresponds to the average grain size in the sediment prior to compaction and quartz cementation. The grain size of the sediment precursor of the Fontainebleau sandstone can be inferred from sieve analysis and examination of thin sections to distinguish cement overgrowths from original grains; the average grain size is found to be 200 μm.

Using this grain size, the model matches the permeability/porosity trend of 240 samples reported by Bourbie and Zinszner (1985), Figure 4. Though the permeabilities span nearly five orders of magnitude, the average error is only 49%. Most of this error occurs in low-porosity samples: the average error for samples of porosity <0.05 is 100%, while the average error for samples of porosity >0.05 is 23%. Minor scatter is observed among samples of the same porosity. This scatter and the discrepancies between the predictions and measurements can be attributed to the fact that the rock grains are not spherical and exhibit a variable (though narrow) distribution of sizes, rather than a single size. In particular, samples having low porosity tend to have original grain sizes smaller than 200 μm, accounting for our overestimation of permeability in some of

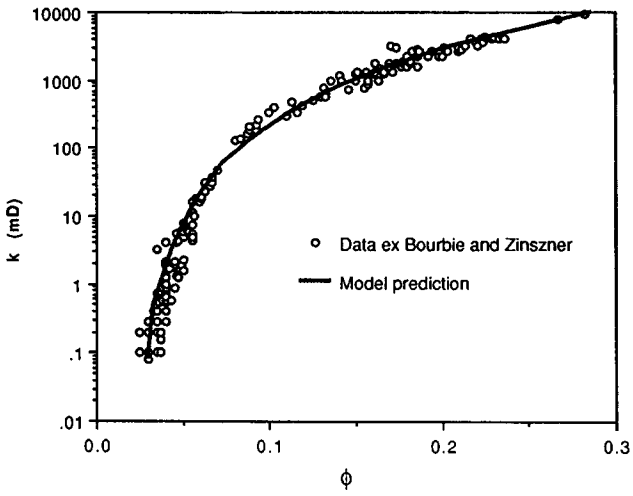

Figure 4. Comparison of permeability/porosity trend predicted by the model with measurements on samples of Fontainebleau sandstone reported by Bourbie and Zinszner (1985).

The agreement is obtained without adjustable parameters and without correlations involving additional measurements.

these samples. We emphasize that despite this, agreement over the entire range of values is obtained without adjustable parameters and that no additional measurements were made on any samples. The predictions are calculated exclusively from the microgeometry of the model porous media, which in turn is defined by simulated physical processes. In contrast, many previous methods of predicting permeability using network models would require detailed measurements (for example, pore image analysis or mercury injection) of the pore structure in many samples. The number of samples involved would make this a lengthy project.

Because the network model is physically representative, it affords useful physical insights. For example, consider the change in the slope of the permeability/porosity trend at around 10% porosity. Bourbie and Zinszner (1985) observed that permeability followed one power law relationship with porosities exceeding 10%, but a different power law for porosities less than 10%. They hypothesized that pore throat blocking was responsible for the different relationships. Our model provides physical evidence in support of this hypothesis. As shown in Figure 3, throat blocking becomes significant when compaction/grain growth reduces the porosity to around 10%. As a result, more and more routes (sequences of individual flow paths) for flow through the medium become disconnected as porosity decreases below 10%. For porosity greater than 10%, permeability declines primarily because compaction/cementation shrinks pore throats. For porosity less than 10%, throat shrinking continues, but its effect is reinforced by the loss of flow routes. Consequently, the permeability declines more rapidly. Because porosity measures all void space without regard to connectivity, a single power law in porosity cannot fit the permeability trend. For the same reason, the electrical conductivity of the pore space of these media (the grains are assumed to be insulators) exhibits a similar though less pronounced effect (Roberts and Schwartz, 1985; Doyen, 1988).

Recall that the network model used here automatically incorporates spatial correlation at the pore scale. If we instead use only the frequency distribution of conductivities, as in an effective medium theory or stochastic network calculation of permeability, the predictions uniformly overestimate the measurements (cf. Figure 2). The average error in predictions made from uncorrelated (that is, randomized) networks having the correct frequency distribution of conductivities is 6,995% in samples having porosity <0.05 and 488% in samples having porosity >0.05. The size of the error for low-porosity samples reflects the fact that the randomized networks continue to percolate beyond the threshold of the physically representative networks. The error in predictions made from effective medium theory is 286%. This error is smaller than that of the random networks because the effective conductivity tracks permeability correctly near the percolation threshold (porosity ~ 0.03). This is a fortuitous consequence of the fact that 50% of the pore throats are blocked at the percolation threshold in the physically representative networks. (The effective medium conductivity in an uncorrelated four-connected network vanishes when half the bonds are blocked, even though such a network continues to percolate until about 61% of the bonds are blocked.) The predictions obtained from uncorrelated frequency distributions of conductivities are significantly worse than predictions from the physically representative networks. The agreement with the spatially correlated model supports our assertion that spatial correlation is inherent in granular porous media.

Discussion

These results indicate that direct simulation of the results of physical processes is a powerful method for predicting properties of the media created by those processes. An obvious question is how far this approach can be extended. We have simulated other geological phenomena such as precipitation of carbonate minerals and certain clay minerals and found good agreement with measurements. However, when the sediment contains a wide distribution of grain sizes, our method of obtaining a network representation is not well suited to defining pore throats for fluid flow. The same difficulty arises when calculating electrical conductivity (Schwartz and Banavar, 1989). We are developing alternative methods for this case.

It seems probable that more complex natural systems (such as most sedimentary rocks) would exhibit even more spatial correlation than the simple model porous media considered here. This is because our starting point is an isotropic collection of isotropic particles (spheres). Real sediments are deposited under anisotropic fields (such as gravity) and are composed of anisotropic particles. The location and the orientation of such particles will be influenced by the location and orientation of neighboring particles in the sediment, as well as by the directions of the fields. Network models that account for spatial correlation would be more representative of the pore space in such media and thus could provide better physical insight into transport through the media.

Since the structure of the model porous media is completely specified, other structure-dependent properties such as relative permeability (Bryant and Blunt, 1992), acoustic velocity, diffusivity and pore-space electrical conductivity can be calculated directly and independently. We have also applied the method of Mason and Mellor (1991) to simulate mercury porosimetry

in this class of media. The results agree both quantitatively and qualitatively with measurements reported by Bourbie and Zinszner. The results of the electrical calculations agree with those of Roberts and Schwartz (1985); the procedures differ in that we do not use any "free scaling parameter." Our prediction of acoustic velocity circumvents the long-standing problems of measuring frame moduli and pore aspect ratio distributions. We will describe such calculations in future publications.

Conclusions

We have simulated the results of processes that create a simple two-parameter class of porous media. The processes are sedimentation (creation of a dense, disordered packing of monodisperse grains), compaction (reduction of the bulk volume of the packing by mechanical compression), and grain growth (increase in grain radii without moving grain centers). The simulation is carried out so as to yield physically representative models whose structures are completely specified. Network models that preserve the topology and geometry of the pore space are then extracted from these structures. These models permit direct calculation of transport through the porous media over a range of degrees of compaction and grain growth.

Permeability predictions from the models match measurements on Fontainebleau sandstone samples whose permeabilities span nearly five orders of magnitude. No adjustable parameters enter the permeability calculation. No additional measurements, such as mercury porosimetry or thin section analysis, are necessary. No correlations between permeability and other properties are used.

The geometry of the pore space in this class of granular media is spatially correlated at the pore scale. This departure from independent statistics significantly influences permeability, in accordance with previous results for other macroscopic properties (electrical conductivity, percolation threshold). Artificially removing the correlation increases permeability by as much as an order of magnitude. The success of the model predictions indicates that spatial correlation is intrinsic to real granular media. Uncorrelated models of such media are therefore unlikely to be physically representative. We hold the suspicion that many natural systems are strongly spatially correlated at the pore scale.

Acknowledgment

BP Exploration supported this work and permitted its publication. We are grateful to Professor J. L. Finney for permitting access to his sphere packing coordinates. Jonathan Evans determined the grain size of samples of Fontainebleau sandstone and assisted with the network model calculations.

Notation

g_{ij} = hydraulic conductivity of a flow path between adjacent sites i and j
k = permeability of porous medium or network
k_0 = permeability of network representation of Finney's original packing
P_i = pressure in network site i
$\langle P \rangle$ = average pressure at radial distance r from the center of the network
q_{ij} = flux through the flow path between adjacent sites i and j
Q = steady-state flow rate through network
r = radial distance from center of network
r_{eff} = effective radius of a flow path between adjacent cells
r_{eq} = equivalent radius corresponding to the cylindrical tube whose cross-section has the same area as the void in a cell face
r_{ins} = inscribed radius corresponding to the largest cylindrical tube that will fit through the void area in a cell face
R_i = radius of the ith sphere before incremental grain growth
R_i' = radius of the ith sphere after incremental grain growth
R_0 = radius of a sphere in Finney's original packing
x_j = jth coordinate axis for Finney's original measurements of sphere center locations
x_j' = rescaled jth coordinate axis
x_{j_0} = arbitrary reference value on jth coordinate axis
z = effective length of a flow path between adjacent cells

Greek letters

ΔR = parameter for increasing radii of spheres in packing to simulate grain growth
ϕ = porosity
λ = parameter for rescaling coordinate axis to simulate compaction
μ = fluid viscosity

Literature Cited

Alvfors, P., and G. Svedberg, "Modelling of the Simultaneous Calcination, Sintering and the Sulphation of Limestone and Dolomite," *Chem. Eng. Sci.*, **47**, 1903 (1992).
Bourbie, T., and B. Zinszner, "Hydraulic and Acoustic Properties As a Function of Porosity in Fontainebleau Sandstone," *J. Geophys. Res.*, **90**, 11524 (1985).
Bryant, S., and M. Blunt, "Prediction of Relative Permeability in Simple Porous Media," *Phys. Rev. A*, **46**, 2004 (1992).
Bryant, S., P. King, and D. Mellor, "Network Model Evaluation of Permeability and Spatial Correlation in a Real Random Sphere Packing," to appear in *Transport in Porous Media* (1993).
Chu, C., and K. Ng, "Flow in Packed Tubes with a Small Tube to Particle Diameter Ratio," *AIChE J.*, **35**, 148 (1989).
Chung, G., B. McCoy, J. Smith, D. Cagliostro, and M. Carswell, "Chemical Vapor Infiltration: Modelling Solid Matrix Deposition in Ceramic-Ceramic Composites," *Chem. Eng. Sci.*, **46**, 723 (1991).
Currier, R., "Overlap Model for Chemical Vapor Infiltration of Fibrous Yarns," *J. Amer. Ceram. Soc.*, **73**, 2274 (1990).
De Cayeux, M., C. Gauthier, Y. Lévy, N. Tran, and F. Delyon, "Assessing Some Aspects of Deep Bed Filtration of Clay Suspensions via Transport Properties," *Powder Tech.*, **62**, 183 (1990).
Doyen, P., "Permeability, Conductivity and Pore Geometry of Sandstone," *J. Geophys. Res.*, **93**, 7729 (1988).
Dullien, F., and G. Dhawan, "Bivariate Pore-Size Distribution of Some Sandstones," *J. Coll. Interf. Sci.*, **52**, 129 (1975).
Ehrlich, R., S. Kennedy, J. Crabtree, and R. Cannon, "Petrographic Image Analysis: I. Analysis of Reservoir Pore Complexes," *J. Sedim. Petrol.*, **54**, 1365 (1984).
Elam, W., A. Kerstein, and J. Rehr, "Critical Properties of the Void Percolation Problem for Spheres," *Phys. Rev. Lett.*, **52**, 1516 (1984).
Fatt, I., "The Network Model of Porous Media," *Petrol. Trans. AIME*, **207**, 144 (1956).
Fernandez, J., P. Duran, and C. Moure, "Dielectric and Microstructural Properties of Sintered $BaTiO_3$ Ceramics Prepared from Different TiO_2 Raw Materials," *J. Mat. Sci.*, **26**, 3257 (1991).
Finney, J., "Random Packings and the Structure of the Liquid State," PhD Thesis, Univ. of London (1968).
Finney, J., "Random Packings and the Structure of Simple Liquids: I. The Geometry of Random Close Packing," *Proc. Roy. Soc.*, **319A**, 479 (1970).
Koplik, J., C. Lin, and M. Vermette, "Conductivity and Permeability from Microgeometry," *J. Appl. Phys.*, **56**, 3127 (1984).
Lange, F., L. Atteraas, F. Zok, and J. Porter, "Deformation Consolidation of Metal Powders Containing Steel Inclusions," *Acta Metall. Mat.*, **39**, 209 (1991).
Lange, F., and B. Kellett, "Thermodynamics of Densification: II. Grain Growth in Porous Compacts and Relation to Densification," *J. Amer. Ceram. Soc.*, **72**, 735 (1989).

Lin, C., and M. Cohen, "Quantitative Methods for Microgeometric Modeling," *J. Appl. Phys.*, **53**, 4152 (1982).
Mason, G., and D. Mellor, "Analysis of the Percolation Properties of a Real Porous Material," *Characterization of Porous Solids II*, p. 41, F. Rodriguez-Reinoso et al., eds., Elsevier Science Publishers, Amsterdam (1991).
Mellor, D., "Random Close Packing (RCP) of Equal Spheres: Structure and Implications for Use As a Model Porous Medium," PhD Thesis, Open Univ., Milton Keynes, U.K. (1989).
Mishra, B., and M. Sharma, "Measurement of Pore Size Distributions from Capillary Pressure Curves," *AIChE J.*, **34**, 684 (1988).
Payatakes, A., C. Tien, and R. Turian, "A New Model for Granular Porous Media: I. Model Formulation," *AIChE J.*, **19**, 58 (1973).
Rege, S., and H. Fogler, "A Network Model for Deep Bed Filtration of Solid Particles and Emulsion Drops," *AIChE J.*, **34**, 1761 (1988).
Ripley, B., *Spatial Statistics*, p. 42, Wiley, New York (1981).
Roberts, J., and L. Schwartz, "Grain Consolidation and Electrical Conductivity in Porous Media," *Phys. Rev. B*, **31**, 5990 (1985).
Rubinstein, J., and S. Torquato, "Flow in Random Porous Media: Mathematical Formulation, Variational Principles, and Rigorous Bounds," *J. Fluid Mech.*, **206**, 25 (1989).
Sahimi, M., G. Gavalas, and T. Tsotsis, "Statistical and Continuum Models of Fluid-Solid Reactions in Porous Media," *Chem. Eng. Sci.*, **45**, 1443 (1990).
Schlueter, E., N. Cook, P. Witherspoon, and R. Zimmerman, "Predicting Permeability and Electrical Conductivity of Sedimentary Rocks from Microgeometry," paper T21E-12, *EOS Trans. Amer. Geophys. Union*, **71**, 1586 (1990).
Schwartz, L., and S. Kimminau, "Analysis of Electrical Conduction in the Grain Consolidation Model," *Geophys.*, **52**, 1402 (1987).
Schwartz, L., and J. Banavar, "Transport Properties of Disordered Continuum Systems," *Phys. Rev. B.*, **39**, 11965 (1989).
Sotirchos, S., and S. Zarkanitis, "Pellet-Model Effects on Simulation Models for Fixed-Bed Desulfurization Reactors," *AIChE J.*, **35**, 1137 (1989).
Spearing, M., and G. Matthews, "Modelling Characteristic Properties of Sandstones," *Transport in Porous Media*, **6**, 71 (1991).
Sung, G., C. Carter, D. Cho, and C. Kim, "Sinter-Forged $YBa_2Cu_3O_{7-x}$ Superconducting Ceramics from the Spray-Roasted Powders," *J. Mat. Sci.*, **26**, 1803 (1991).
Tai, N.-H., and T.-W. Chou, "Modeling of an Improved Chemical Vapor Infiltration Process for Ceramic Composites Fabrication," *J. Amer. Ceram. Soc.*, **73**, 1489 (1990).
Taylor, S., P. Milly, and P. Jaffé, "Biofilm Growth and the Related Changes in the Physical Properties of a Porous Medium: 2. Permeability," *Water Res. Res.*, **26**, 2161 (1990).
Vandermeer, R., R. Masumura, and B. Rath, "Microstructural Paths of Shape-Preserved Nucleation and Growth Transformations," *Acta Metall. Mat.*, **39**, 383 (1991).
Wardlaw, N., Y. Li, and D. Forbes, "Pore-Throat Size Correlation from Capillary Pressure Curves," *Transport in Porous Media*, **2**, 597 (1987).
Yanuka, M., F. Dullien, and D. Elrick, "Percolation Processes and Porous Media: I. Geometrical and Topological Model of Porous Media Using a Three-Dimensional Joint Pore Size Distribution," *J. Coll. Interf. Sci.*, **112**, 24 (1986).
Yu, H.-C. and S. Sotirchos, "A Generalized Pore Model for Gas-Solid Reactions Exhibiting Pore Closure," *AIChE J.*, **33**, 382 (1987).

Appendix: Network Model Representation of Pore Space in Simple Granular Porous Media

The text describes the construction of consolidated porous media from a real random packing of monodisperse spheres. The media are characterized by the degree of compaction (λ in Eq. 1) and the extent of grain growth (ΔR in Eq. 2). Here we describe the extraction of a network model of the pore space in these media, from which we calculate permeability. This discussion summarizes the essential features of more detailed reports published elsewhere (Bryant et al., 1993; Mellor, 1989).

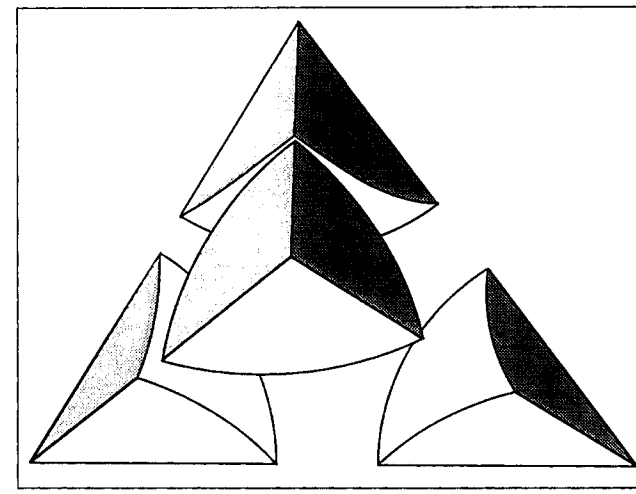

Figure 5. A tetrahedral cell from a Delaunay tessellation of sphere centers in a random dense packing.

The corners of the tetrahedron are the centers of four nearest neighbor spheres. Prior to compaction and grain growth, the edges of the cell must have lengths of at least 1.0 sphere diameters. Because the spheres are disordered, rather than regularly packed, the cell is irregular.

Defining pore bodies and pore throats

An unambiguous method of defining discrete pores within the packing is required for each value of λ and ΔR. We adopt the method of Mellor (1989) and tessellate the packing volume into tetrahedra known as Delaunay cells (Ripley, 1981). [Chu and Ng (1989) used a similar tessellation to study wall effects in flow through computer-generated packed tubes.] Delaunay cells group nearest neighbor spheres together in the packing. The centers of the nearest neighbor spheres define the corners of a cell, as shown in Figure 5. (Four spheres are nearest neighbors if the circumsphere defined by their four centers does not encompass the center of any other sphere in the packing).

The void area in a face of a cell in a sphere pack corresponds to a local minimum in the cross-sectional area. Hence, in a capillary drainage process such as mercury intrusion, the faces control access to the interior of the cell. The faces, therefore, correspond naturally to pore throats, while the cell interior corresponds to a pore. Mason and Mellor (1991) took advantage of this feature of the cells to study drainage and imbibition in the Finney packing. Because the Delaunay cells subdivide the packing volume completely and without overlap, the porosity of the packing at any ΔR and λ is readily calculated as the total void volume of the cells divided by the total cell volume.

Network topology

The tessellation of the packing into tetrahedral cells can be represented as a network of sites and bonds, as shown in Figure 6. The sites correspond to the cells themselves, and the bonds are links between cells that share a common face. It is convenient to assign a spatial location to the sites, and the natural choice for this location is the geometric center of the cell (that is, the point equidistant from the centers of the four spheres defining the cell). A bond then corresponds to the flow path

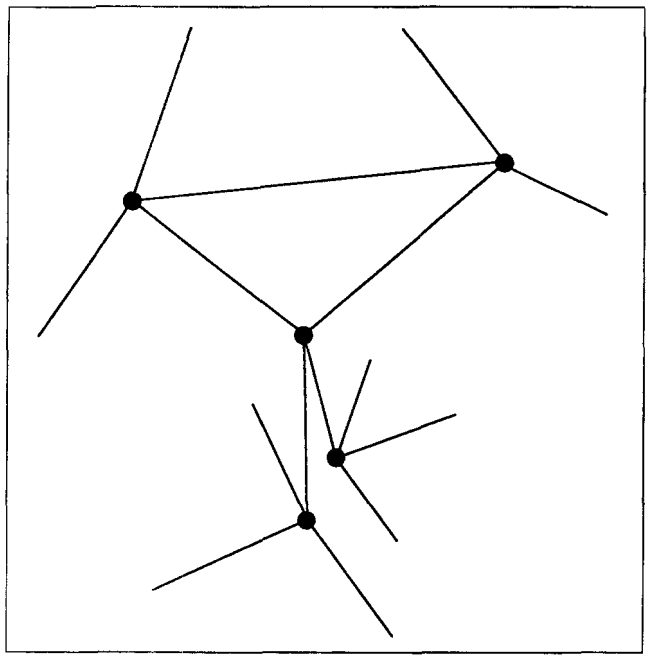

Figure 6. Part of the network showing how several adjacent cells in the tessellation of the sphere packing are connected.

The sites represent cells (pores); the bonds link cells that share a common face and thus correspond to pore throats (flow paths). Every site has four bonds, a consequence of the fact that every cell is a tetrahedron.

that connects the centers of adjacent cells. This path passes through the common face shared by adjacent cells. In the present work we use the central core of 3,367 spheres in Finney's packing, from which a network of about 15,000 sites and about 30,000 bonds is obtained.

Since each cell is a tetrahedron, the coordination number of the network is constant: each site has four bonds. Thus, the method of defining pores establishes a physical basis for the network topology; the coordination number is not an adjustable parameter. Although the coordination number is uniform, the network itself is completely disordered; it exhibits no regions of crystallinity (Roberts and Schwartz, 1985; Mellor, 1989).

Network geometry

The geometry of each flow path (bond in the network) is fixed by the geometry of the cells joined by the flow path. Hence, we can calculate the hydraulic conductivity of each flow path directly. The following is a summary of the procedure; a full description appeared in Bryant et al. (1993). In analogy with the Hagen-Poiseuille law for tubes, the hydraulic conductivity between cells i and j may be expressed as:

$$g_{ij} = \pi\, r_{\text{eff}}^4 / 8\mu z \tag{A1}$$

where r_{eff} and z are the effective radius and length, respectively, of the flow path, and μ is fluid viscosity. The natural definition for the length of a flow path is the distance between cell centers joined by the path. In general, the flow paths have nonzero effective radii, so under this definition of path length the four paths terminating at a cell center will overlap in the vicinity of the cell center. This overlap causes the actual path lengths to be double-counted and thus systematically underestimates the true conductivity. It is straightforward to introduce a correction that largely eliminates the overlap and the associated error in path conductivities.

In a packing of equal spheres, the effective radius of the flow path is closely approximated by the mean of the inscribed and equivalent radii in the cell face through which the path passes:

$$r_{\text{eff}} = (r_{\text{ins}} + r_{\text{eq}})/2 \tag{A2}$$

The inscribed radius r_{ins} is the radius of the largest cylindrical tube that will fit through the cell face; the equivalent radius r_{eq} is the radius of the cylindrical tube whose cross-section has the same area as the void in the cell face. The cross-section of a flow path varies with distance from the cell face, which necessitates a correction to r_{eff}. However, our principal interest is the evolution of permeability during compaction and grain growth. Thus, we will normalize permeability to its value in the uncompacted, uncemented packing, which is 0.0027 (sphere radii)^2 (Bryant et al., 1993). A check showed that the permeability thus normalized is essentially independent of the correction for cross-sectional variation. Hence, we only have to calculate the correction once (in the original Finney packing).

The effective radius and length of each path, and the algorithms to correct them, depend exclusively on the sizes of the cells joined by the path. The cell sizes in turn depend only on Finney's measured sphere center coordinates, so the conductivities of the flow paths involve no adjustable parameters.

Flow through the network

The steady-state pressure distribution in the network follows from the usual Kirchoff's law considerations. Mass is not permitted to accumulate at any site, and flow through a bond is equal to the product of the bond conductivity and the pressure drop between the sites (i and j) connected by the bond:

$$q_{ij} = g_{ij}(P_i - P_j) \tag{A3}$$

The resulting set of equations is solved by Gauss-Seidel successive overrelaxation. The permeability of the network follows from the steady flow rate through the network. Because the overall portion of Finney's original pack that we use here is roughly spherical, it is convenient to impose a spherically symmetric pressure gradient on the network. The spherical form of Darcy's law is given by:

$$\mu Q = 4\pi\, k\, d\langle P\rangle / d(1/r) \tag{A4}$$

where μ is the fluid viscosity, Q is the steady state flow rate out of the packing, k is permeability, and $\langle P\rangle$ is the average pressure of sites contained in a thin spherical shell of radius r; the center of the shell coincides with the central site of the network.

When the packing is numerically compacted in one direction, it becomes anisotropic. The permeability in the compaction direction exceeds the permeability in the transverse directions,

because compaction reduces the lengths of flow paths aligned with the direction of compaction and shrinks the radii of flow paths aligned perpendicular to the compaction direction. This result may surprise readers familiar with sandstones, in which vertical permeability is often much smaller than horizontal permeability. In such sandstones factors such as bedding, lamination and anisotropic grains outweigh the effects observed in our model media.

Our network calculation is carried out in a spherical subset of the compacted packing and thus gives an average of the directional permeabilities. In an extreme case ($\lambda = 0.7$), the permeability in the direction of the axis of compaction is about twice the permeability in the transverse directions. Our primary concern is with geological permeability/porosity trends that span several orders of magnitude, so for this purpose little information is lost by using this average.

The series of calculations described above can be carried out at any values of λ and ΔR. The sphere center coordinates are determined by Finney's original measurements and Eq. 1, while the sphere radii are determined by Eq. 2. This information completely determines the tessellation into cells, which determines the topology and the geometry of the network of flow paths.

Manuscript received Dec. 20, 1991, and revision received July 13, 1992.